ISSN 2303-4521
Periodicals of Engineering and Natural Sciences *Original Research*
Vol. 11, No. 1, February 2023, pp.223-238

Structural behavior of reinforced concrete pre-stressed tapered beams

Mohammed Dhaher Jasim[1], Hayder Talib Nimnim[2]
[1,2]University of Kufa, Engineering Faculty, Iraq

ABSTRACT

This research is focused on studying the flexural behavior of reinforced concrete prestressed (post-tensioned) tapered beams. The present study investigates the impact of compressive strength, prestressed reinforcement, and tapering ratio on flexural behavior. All tested beams have a total length equal to (2600mm) and a clear distance between supports equal to (2400mm), the width of the beam (250mm), and maintain the same amount of concrete volume. The experimental results showed that when a prestressed reinforcement changes from (one strand) for (two strands), this change will affect the prismatic beam, in which the first cracking and the ultimate load will be raised by (60% and 31.71%), respectively, and for a non-prismatic beam with tapering ratios of (1.5 and 2), the first cracking will increase by (12.5% and 2.63%) also the maximum load raised by (28.3% and 31.03%). The failure mode was flexural for all tested beams with crushing in the compression zone. This paper simulated a numerical analysis of experimentally tested specimens using a nonlinear finite element technique (ABAQUS/CAE 2021 software). The numerical outcomes revealed a good correlation compared with the results of the experimental study.

Keywords: Prismatic beams, tapered beams, post-tensioned, concrete type-1 (f'c=40MPa), concrete type-2 (f'c=55MPa), and ABAQUS.

Corresponding Author:

Mohammed Dhaher Jasim
University of Kufa, Engineering Faculty, Civil department, Iraq
Email: mohammedd.albedairy@student.uokufa.edu.iq

1. Introduction

A tapered beam is usually used for buildings with mid-depth frames and in bridges that are simple support or continuous as a double-cantilever lateral beam with a hammerhead. One of the primary prevalent structural components with a non-prismatic shape are haunches that come in parabolic, tapered, or stepped forms. Utilizing concrete beams that are not prismatic allows the cost-effective elimination of steel and concrete if modified to create an element with equivalent strength [1]. Tapered beams have several advantages over prismatic beams, such as cost savings, greater economic efficiency, and aesthetic reasons [2] . Also, shear-carrying achievement can be superior, especially at the joints and support points with another element, an aspect of paramount importance when designing for earthquakes [3]. The purpose of post-tensioning represents to put the concrete structure within the effect of compression at places where load leads to tensile stress. The post-tensioning technique will apply compressive stress to the material, which reduces the tensile stress that may occur when the concrete is loaded. Post-tensioning has been performed through the utilization of tendons by a comprehensive system that includes assembling prestressing steel strands or bars of very high strength. Post-tensioning has been utilized widely in bridges, floor slabs, silos, storage containers, stadiums, nuclear storage containers, Oil rig gravity bases, wind turbines, and constructions pertaining to aesthetics [4]. Post-tensioning elements have advantages such as allowing the designers to take advantage of the concrete's compressive strength and avoid its weak point under tension, reducing or eliminating shrinkage cracking. Therefore, no or fewer joints are required, and in the event of a crack

forming, it is tightly sealed [5]. Archundia-Aranda et al., (2013) found that non-prismatic beams exhibit more remarkable deformation ability in shear compared to prismatic beams and can disperse more energy or an equal amount of energy dispersed by prismatic beams [6]. Godínez-Domínguez et al., (2015) attempted to assess the ability and limitations of analytical for both simple and complex models for predicting the structural behavior of non-prismatic (haunched) beams of reinforced concrete that fail in shear. Their results clarified that the numerically measured cracks were larger than the experimentally determined, and sometimes the cracking reached regions where cracking had not been physically seen [7]. Shuo et al., (2019) demonstrated that the capacity for shearing and the contribution of stirrups was not significantly elevated by the rise in the ratio of stirrups, and the state of the shear resistance mechanism differed due to varying stirrup arrangements for tapered short reinforced concrete beams [8] . Park et al., (2016) found that many values of stress in strands of high strength and deformed rebars subjected to a full-service load were slightly higher than ACI 318 permissible limits [9]. Hou et al., (2017) attempted to clarify the mechanism of shear resistance of reinforced concrete and concrete prestressed with tapered shape beams that do not have stirrups and discovered that the prestress level increased when the prestressed concrete tapered slender beams without stirrups (a/d = 5.0) and the shear stress flow inclination decreased while the critical section's adequate depth became larger [10].

2. Method

2.1. Description of test beams

In the current study, the experimental work involved ten simply supported beams (seven are tapered, and three are prismatic) were studied to test their flexural behavior. The tapered beams had a total length of 2600 mm, 250 mm in width, a varying depth with (512 and 566) mm for tapering ratios (1.5 and 2) respectively at the middle and decreasing heights of (256 and 283) mm for tapering ratios (1.5 and 2) in order near the support. The prismatic beam spanned (2600) mm in overall length, 250 mm in width, and 430 mm as a constant depth. The amount of mild steel was (2Ø8) mm at the compression zone and (2Ø12) mm for the tension zone for every beam tested. However, concerning transverse reinforcement, the tested beams have various levels of reinforcement depending on the designing procedure and section requirements to ensure a flexural failure. The difference was in a prestressed reinforcement amount which was variable between one and two strands, and also, two beams without strands can be considered non-prestressed specimens. The beams have been tested by being subjected to a two-point loads system. The clear span of all beams is (2400) mm, and the bearing steel plates with dimensions of (100x250x20) mm were used under-points loading and above supports to eliminate local failure. All details of tested specimens shown in Table.1 and Figures (1-7) clarified the reinforcement details.

Table 1. Description of tested specimens

Symbols	Depth at support (h_1) (mm)	Depth at Mid-span (h_2) (mm)	Tapering ratio h_2/h_1	Compressive Strength of Concrete ($f'c$) (MPa)		No. of strands
B1-1	430	430	1	40		1
B1-2						2
B′1-1				55		1
B1.5-0	341.5	512.3	1.5	40		0
B1.5-1						1
B1.5-2						2
B′1.5-1				55		1
B2-0	283		566	2	40	0
B2-1						1
B2-2						2

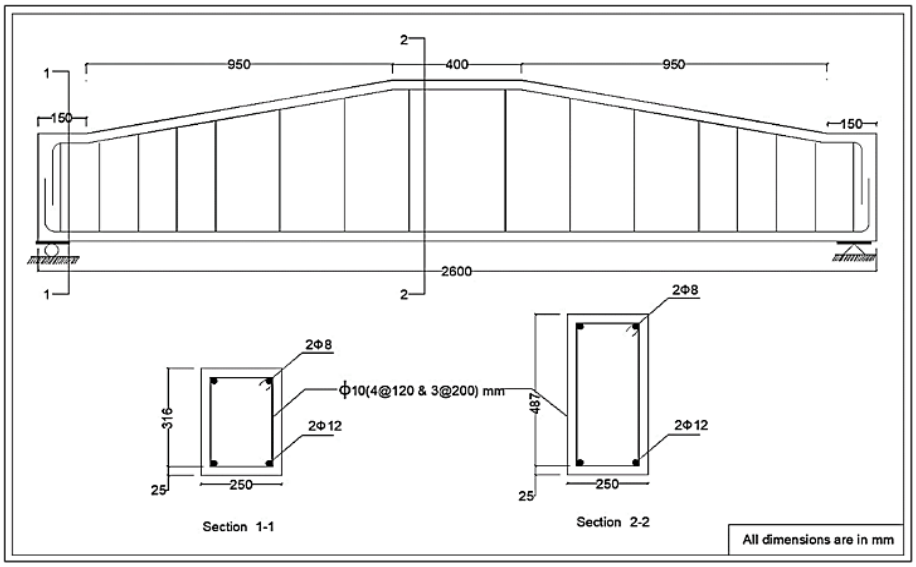

Figure 1. Details of beam B1.5-0

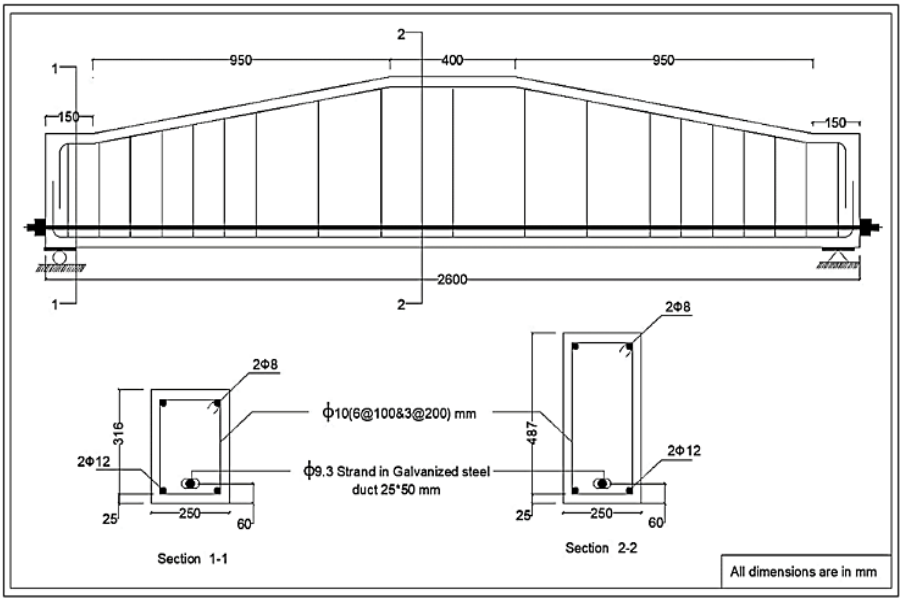

Figure 2. Specifications of the beams B1.5-1 and B'1.5-1

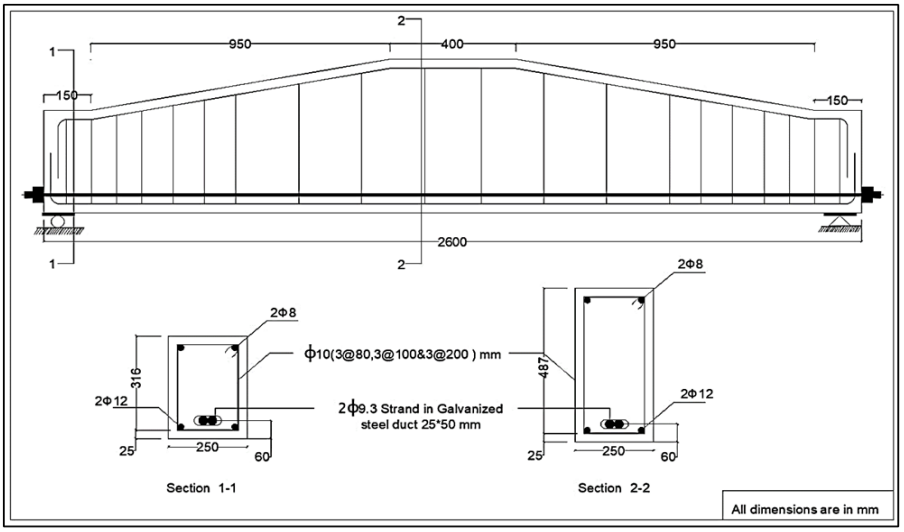

Figure 3. Details of beam B1.5-2

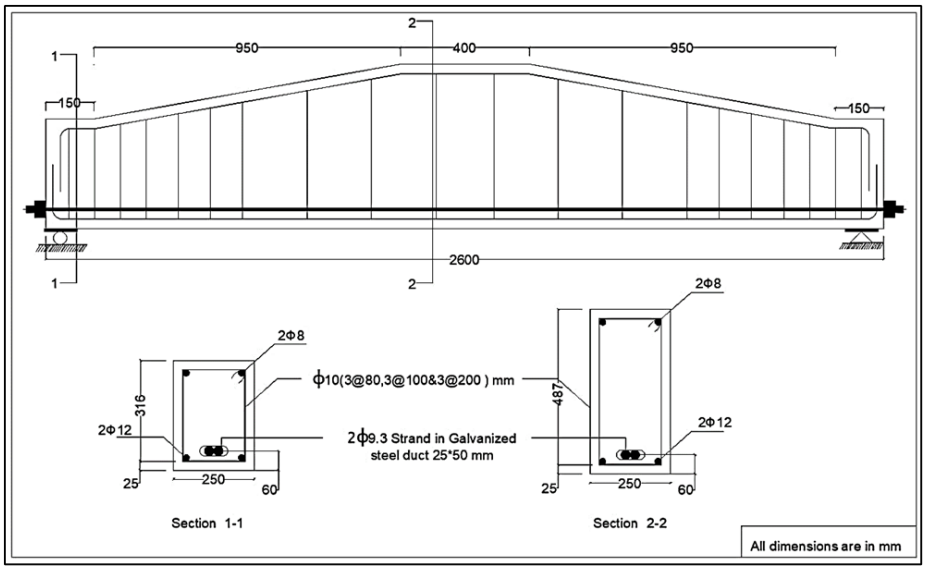

Figure 3. Details of beam B1.5-2

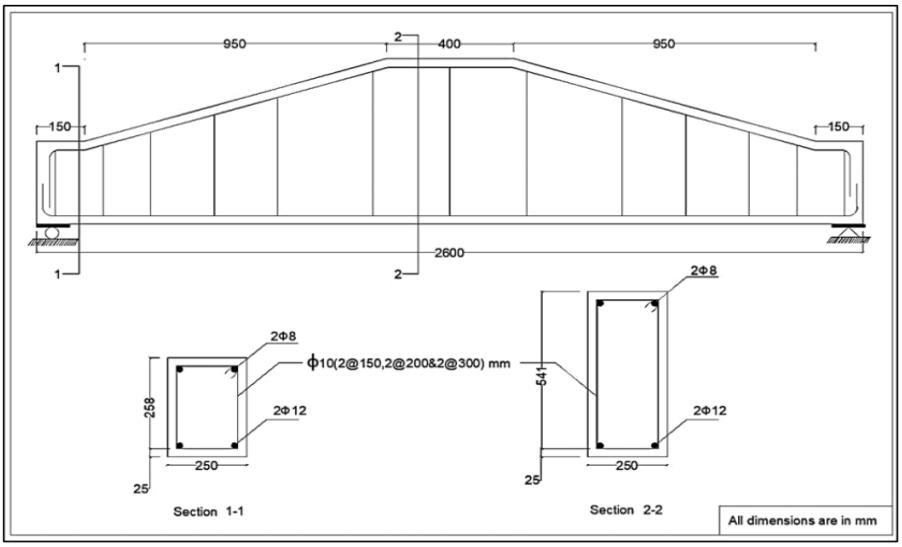

Figure 4. Specifications of the beam B2-0

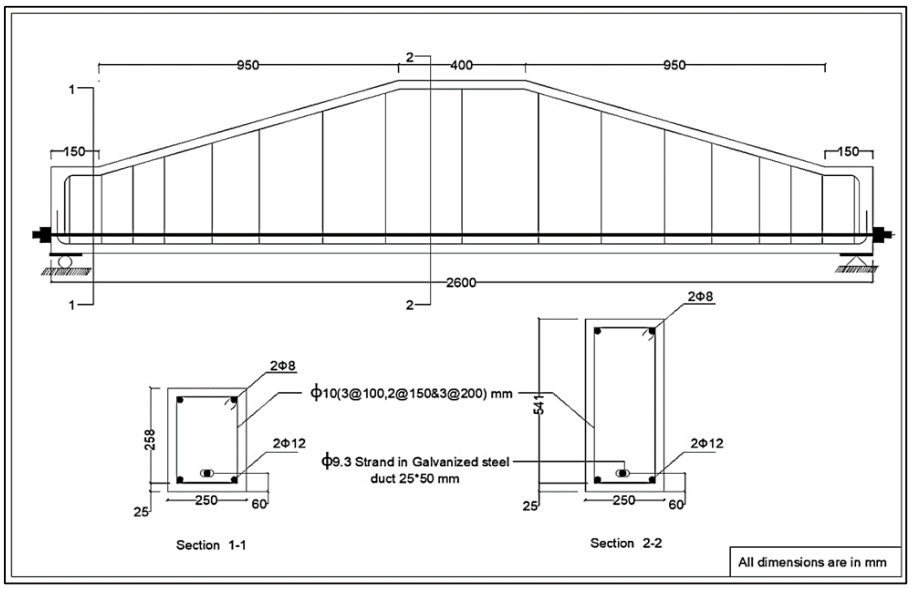

Figure 5. Details of beam B2-1

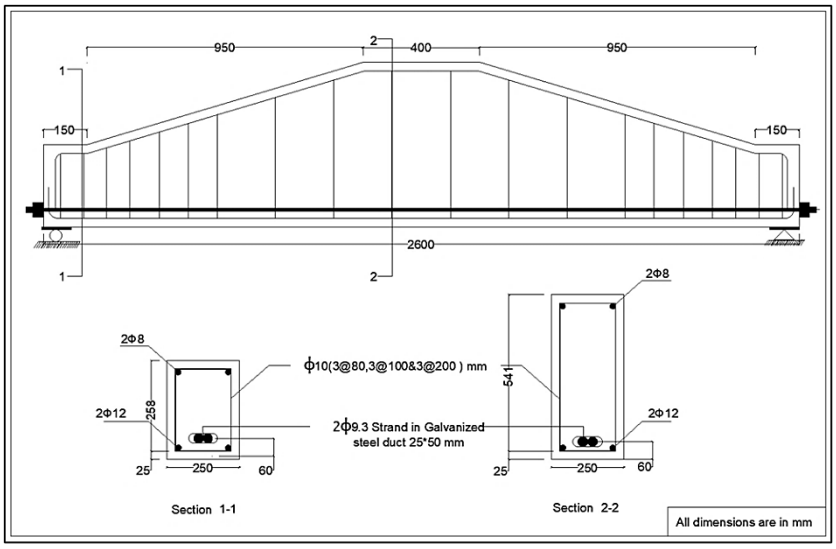

Figure 6. Details of beam B2-2

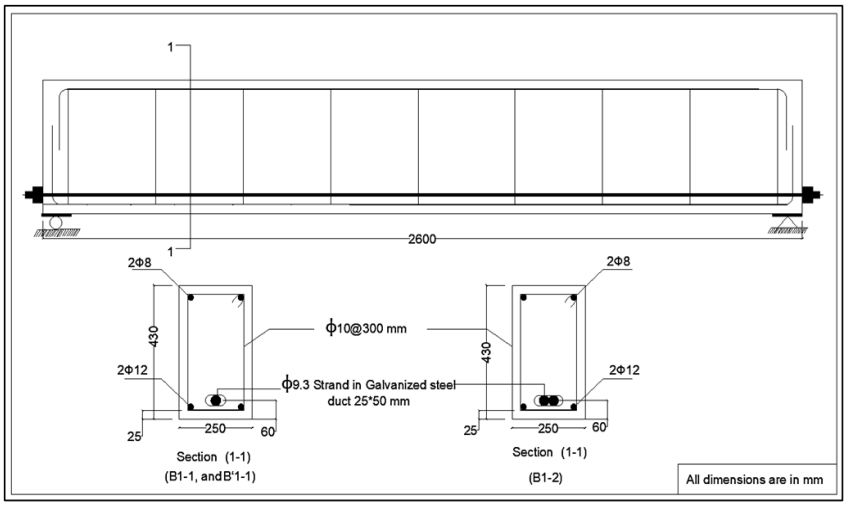

Figure 7. Details of beams B1-1, B'1-1, and beam B1-2

2.2. A non-linear finite element work

For the concrete beam and strand, the model of "an 8-node linear brick, reduced integration, hourglass control element (C3D8R)" was used. The 2-node linear 3-D truss elements were used to model the longitudinal and transverse steel bars (T3D2). The CDP material model in ABAQUS characterizes the typical uniaxial behavior of concrete in tension and compression. Steel is a homogeneous material that can impose the relationship between strain and stress identically on the tensile and compressive sides [11]. Table.2 illustrates the concrete damage plasticity coefficient, and Table.3 clarifies the elastic and plastic characteristics of steel bars and strands. In order to simulate the interaction of a concrete beam and steel bars as longitudinal and stirrups, the "Embedded" option is used to join the rebar with the concrete beam. "Embedded" is a simplistic model for perfect bonding between internal bars and concrete during the theoretical section analyses. The "Contact" constraint is used to simulate the interaction of a concrete beam and steel strands. In contact between strands and concrete, was used a (small-sliding) instead of a (finite-sliding) because it is more sensitive to tracking approach to initial local gaps at the contact interface [12]. Also, a surface-to-surface contact procedure was used for contact between concrete and strand. In contact properties, a "Hard" contact in normal behavior is used to prevent the penetration of strands into concrete [13] [13]. A strand in a post-tensioned manner remains unbounded from the surrounding sheath (duct) at the time of the process of post-tensioning.

The bonding state can be achieved in construction by introducing grout within the strand sheath (duct). This procedure can be simulated in modeling using a contact formulation between the strand and concrete. The grouting mechanism is simulated by "Penalty" with a "friction coefficient" of 0.55. To make a numerical (FEA) on a beam, the analysis process is divided into two main steps, besides the initial step for beams subjected to prestressed force by strands. The following points summarize the loading steps:

1) In the (Initial) step, the boundary condition in the bottom beam was applied, as illustrated in Plates (5-2, a and b).
2) In (Step-2), a prestressed force was applied to strands on one side of a beam as a real experimental test. The applied load is subjected to a reference point connected with the strand end face by (Coupling) interaction. A constraint with (Ux=0, Uy=0, and Uz=0) was applied on the other strand end, as clarified in Plates (5-3, a, b and c). The current step is not found in non-prestressed beams.
3) In (Step-2), the subjected prestressed force on the strand's end was stopped, and a constraint was imposed on the same end using (Ux=0, Uy=0, and Uz=0), at the same experimental condition, as displayed in Plate (5-4).

Table 2. The concrete damage plasticity coefficient

Concrete Damage Plasticity Coefficient	
Dilation Angle	35
Eccentricity	0.1
f_{bo}/f_{co}	1.16
K_c	0.667
Viscosity Parameter	0.001
Poisson’s ratio	0.2
Modulus of elasticity (f'c=40MPa)	29200
Modulus of elasticity (f’c=55MPa)	31400

Table 3. The elastic and plastic characteristics of steel bars and strands.

Diameter of bar	Cross-sectional area (mm^2)	Elastic stage		Plastic stage		
		Modulus of elasticity (MPa)	Poison ratio	Stress (MPa)		Plastic strain
Ø8	50.2	200000	0.3	f_y	470	0
				f_u	684	0.11
Ø10	78.5			f_y	485	0
				f_u	680	0.1
Ø12	113			f_y	490	0
				f_u	684	0.1
Strand Ø9.3	53.8			f_{py}	1800	0
				f_{pu}	1973	0.06

3. Experimental results

At the early loading stage, when tension is controlled at midspan, the first cracks occur at this region, and the load at this stage is known as "cracking load." For flexural failure, cracks appeared in the tension zone, then became wider and propagated toward the compression zone in conjunction with load increasing. Cracks propagated and extended quickly while loading increased. The failure occurred when the compression zone transformed into a crushed area at the maximum load capacity. There is no shear failure because the study concentrated on the flexural behavior of beams, and the beam was strengthened to withstand shear failure adequately. The first crack load, ultimate load, maximum deflection, first crack deflection, and load-deflection curves are discussed, and the results are listed in Table.4.

Table 4. Tested beams results

Beams symbol	Pcr (kN)	Pu (kN)	Δcr (mm)	Δu (mm)	Δs (mm)	Mode of failure
B1-1	50	205	1.35	32.9	6.82	Flexural failure with crushing in compression zone
B′1-1	60	210	1.83	27.54	6.23	
B1-2	80	270	1.6	21.1	6.91	
B1.5-0	50	170	2.08	33.8	7.68	
B1.5-1	80	265	1.94	34.9	8.65	
B′1.5-1	90	270	1.8	29.2	6.52	
B1.5-2	90	340	1.29	36.7	9.31	
B2-0	40	190	1.08	20.52	5.95	
B2-1	80	290	1.9	35.4	8.78	
B2-2	110	380	1.95	42.1	7.98	

3.1. Effect of concrete strength

Curves were plotted to illustrate the relationship between load and deflection (at mid-span) for prismatic and non-prismatic beams. For prismatic beams, it can be noticed by looking at Figure.8 that the curves have converging paths in the initial stages of loading; after that, the beam with the concrete type-2 (55MPa) has deflection less than the beam with the concrete type-1 (40MPa) in all stages because of the difference in stiffness of beams, which leads to the apparent contrast between curves. For non-prismatic beams, the curves have somewhat paths that have a little close together at the elastic stage, and then they have different routes for all stages of loading due to the difference in the stiffness for these beams.

Also, when viewing Figure.8, it was observed that the beams with a concrete type-2 had enhanced their flexural behavior and offered more stiffness, in which its beams deflect at every loading stage less than in comparison with the beams with concrete type-1. Also, it showed a decrease in ultimate deflection by (16.3 and 16.33) %, respectively, for prismatic and non-prismatic beams; this can be attributed to the high resistance of the beams with the concrete type 2, which contributes to minimizing deflection.

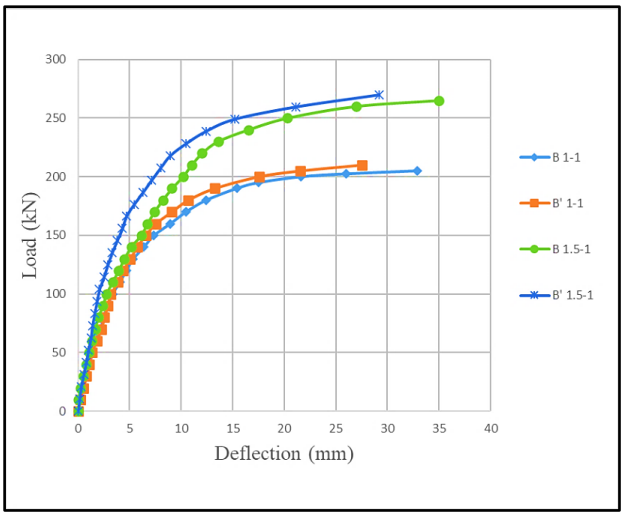

Figure 8. Load-mid span deflection for beams B1-1, B'1-1, B1.5-1 & B'1.5-1

3.2. Effect of prestressed steel reinforcement

A three amount of prestressing reinforcement (number of strands) was employed to evaluate the effect of prestressing reinforcement magnitude on the flexural behavior and failure mode, except for prismatic beams, which have two amounts of prestressing reinforcement. The present study can classify and assess the influence of (number. of strands) depending on a three-group, with every beam of this group containing concrete with a volume equal to each other. Likewise, concerning the rest of the characteristics relevant to tensile and compression, but for a tapering ratio, it varies in each group with a specific value. This part of the discussion can be categorized into three groups in the following order:

Group 1 (Prismatic beams)

In this group of experimental specimens, two prismatic beams (B1-1 and B1-2) with two amounts of prestressing reinforcement (one and two strands), respectively, were exhibited with identical properties and strand locations. It was noted that the ultimate load was increased by (31.7%) in beam (B1-2), which contained a two-strands reinforcement relative to beam (B1-1), which contained one strand. Increasing prestressing reinforcement amounts can increase the resistance toward tensile stress, which develops in response to the external moment. Therefore, the bending moment capacity of the beam goes up, contributing to an increase in the ultimate load. The relationship between load and deflection of the groups' beams is illustrated in Figure.9

Group 2 (Beams with tapering ratio 1.5)

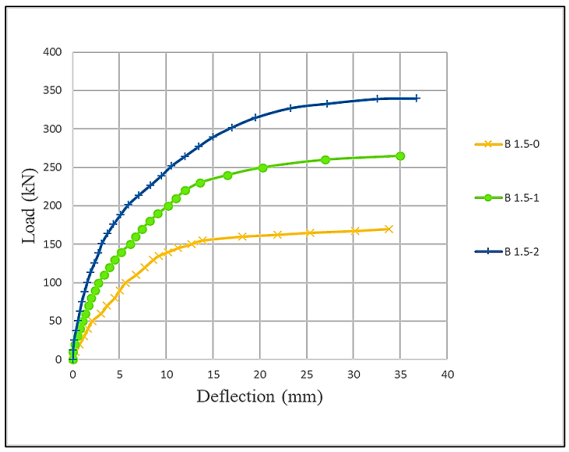

Figure 8. Load-mid span deflection for beams B1-1, B'1-1, B1.5-1 & B'1.5-1

Three non-prismatic beams with a tapering ratio of (1.5) (B1.5-0, B1.5-1, and B1.5-2) serve as target beams to discover the behavior of this group within a specific parametric study involving an increase

in prestressing reinforcement. Three levels of prestressing reinforcement can be denoted by (0, 1, and 2 strands), and the properties and locations of strands are the same. The ultimate flexural strength was improved by substituting two reinforcing strands instead of one and exchanging one strand for none. According to the experimental results, a prestressing reinforcement altered towards value augmentation, affecting the ultimate load capacity and mid-span deflection. The ultimate load was found to be raised by (28.3%) in beam (B1.5-2) with two strands of prestressed reinforcement compared to beam (B1.5-1), which had one strand, and by (55.9%) in beam (B1.5-1) with one strand of prestressed reinforcement compared to beam (B1.5-0), which had no strand (non-prestressed beam). In the same way, when matching the ultimate load capacity of (B1.5-2) with that identified in beam (B1.5-0) can observe an increase of (100%). An increasing the (number of strands) caused improved internal tensile strength due to the development of stresses, which led withstand to resist more external load, thus increasing the ability of the beam to resist external bending moments. The relationship between load and deflection of the groups' beams is shown in Figure10.

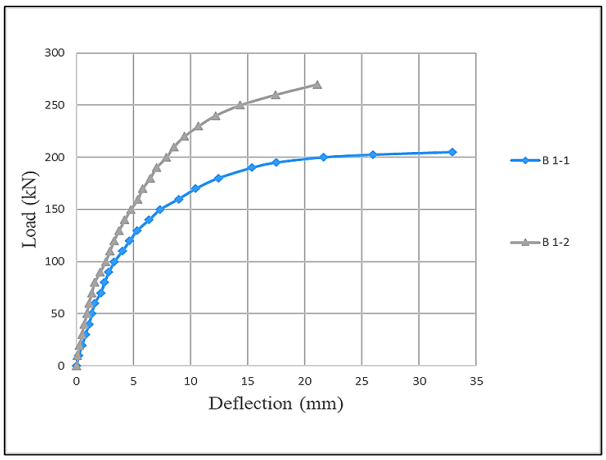

Figure 9. Load-Mid span deflection for beams B1-1 & B1-2

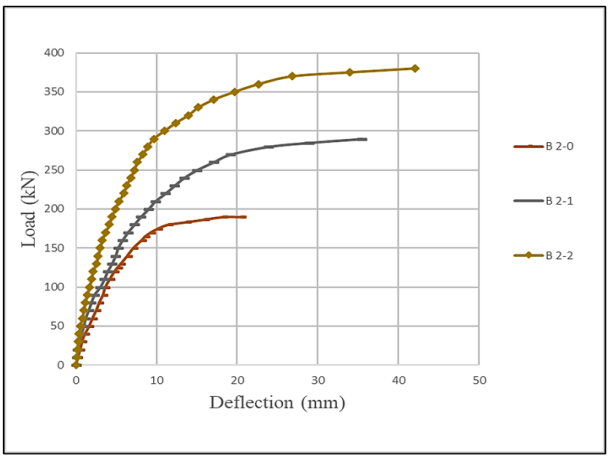

Figure 10. Load-Mid span deflection for beams B1.5-0, B1.5-1& B1.5-2

Group 3 (Beams with tapering ratio 2)

This group consists of three non-prismatic beams with a tapering ratio (2) labeled as (B2-0, B2-1, and B2-2). The provided prestressing reinforcement strands consist of (0, 1, and 2) strands, and the characteristics and strands placement of each beam are the same. The ultimate load in beam B2-2 (with two strands) has been higher than found in B2-1 (with one strand) and B2-0 (without strand), about (31% and 100%), respectively. Furthermore, the ultimate load of (B2-1) was measured and found to be higher (52.63%) than that was detected in the non-prestressed beam (B2-0). The simultaneous intensifying of the prestressed reinforcement (number. of strands) will raise the threshold level of endurance of the developing internal stresses into much-improved status, especially in regions with tensile stress. The relationship between load and deflection of the groups' beams is shown in Figure.11

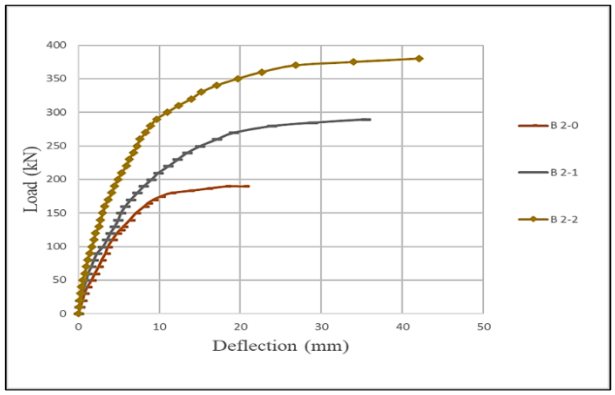

Figure 11. Load-Mid span deflection for beams B2-0, B2-1& B2-2

Effect of tapering ratio: For concrete type-2, it can be noticed from Figure.12 that the ultimate load and deflection increased by (6.01% and 28.57%), respectively, when the tapering ratio raised from 1 (for beam B'1-1) to 1.5 (for beam B'1.5-1).Also, it was observed in Figure.13 that the beam which has a tapering ratio (2) and contains one strand (B2-1) compared with beams (B1.5-1 and B1-1) that contain the same properties of (B2-1) in the amount of prestressed reinforcement and concrete volume except tapering ratio that varied from 1.5 for (B1.5-1) and 1 for (B1-1). The beam (B2-1) can provide a higher ultimate load with (9.43% and 41.46%) compared to the beams (B1.5-1 and B1-1). Thus, it has an ultimate deflection higher by increasing (1.3% and 7.63%) if compared with (B1.5-1 and B1-1) as shown in Figure.4. The beam (B2-2) except the tapering ratio varying from 1 to 1.5 for beams (B1-2 and B1.5-2), respectively. In regard to a beam (B2-2) that has a tapering ratio of (2) with two strands, it gave an ultimate load and maximum deflection larger than beams (B1.5-2 and B1-2) with (11.76% and 40.74%) and (14.6% and 90.5%), respectively, as clarified in Figure 4.

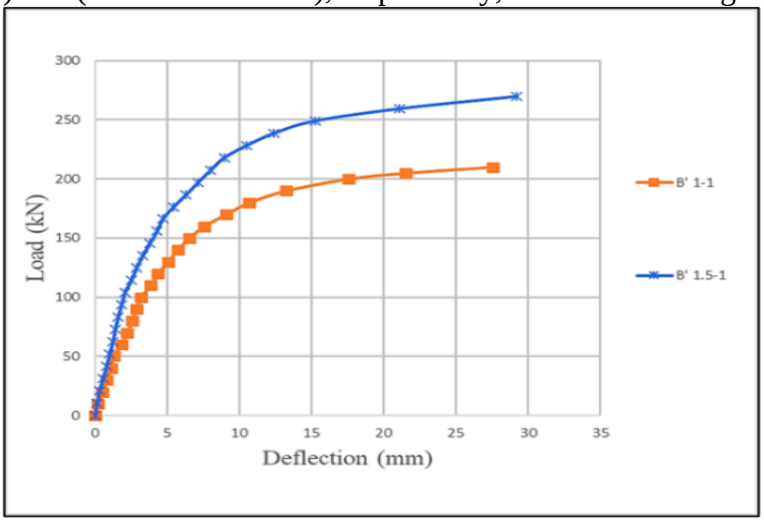

Figure 12. Load-Mid span deflection for beams B'1-1 & B'1.5-1

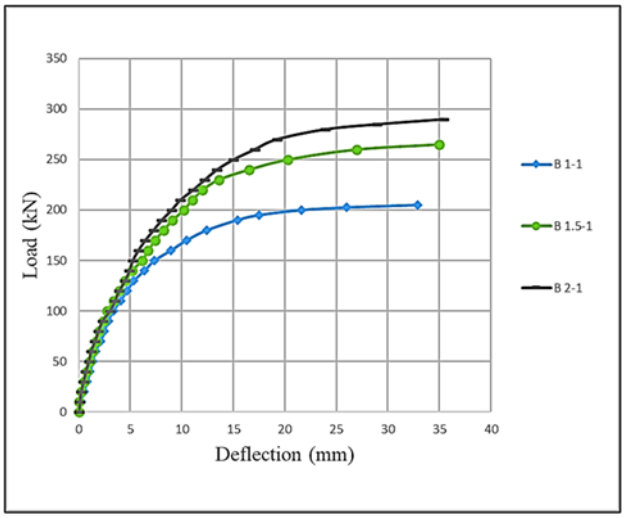

Figure 13. Load-Mid span deflection for beams B1-1, B1.5-1, & B2-1

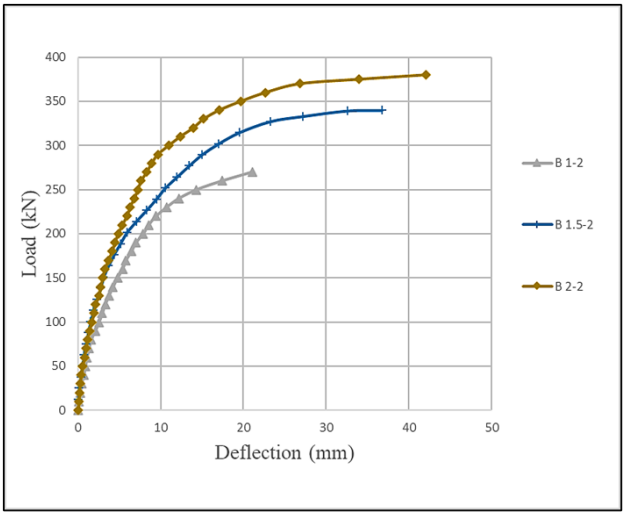

Figure 14. Load-Mid span deflection for beams B1-2, B1.5-2, & B2-2

2.3. Crack patterns and mode of failure

Cracks in concrete generally occur when the tensile stress caused by an applied load is greater than the material's tensile strength. For all tested beams in the present study, it is evident that the cracks are born precisely from the mid-span at the bottom face due to tension dominating. The cracks developed

due to continuous loading and then heading to the upper portion beam and, at the same time, tend towards the compression zone at the top surface in the area between the two-concentrated loads where compression has been governing. Other cracks propagate within the vicinity of the mid-span, along with cracks formed from the beam center towards the constrained region. These cracks appear after the mid-span cracks form and tend toward the compression zone in the top portion of the beams. Crushing in the compression zone between loads happens because of stress development. The failure mode of wholly beams is considered flexural with crunching at the top part of the beams, as illustrated in Plates (1-10).

Plate 1. The failure of the (B1-1) beam

Plate 2. The failure of the (B'1-1) beam

Plate 3. The failure of the (B1-2) beam

Plate 4. The failure of the (B1.5-0) beam

Plate 5. The failure of the (B1.5-1) beam

Plate 6. The failure of the (B'1.5-1) beam

Plate 7. The failure of the (B1.5-2) beam

Plate 8. The failure of the (B2-0) beam

Plate 9. The failure of the (B2-1) beam

Plate 10. The failure of the (B2-2) beam

2.4. Finite element results

The maximum mid-span deflection and a load of failure of (FEA) results for all simulation specimens are shown in Table.5, and Figures (15-24) show the load-deflection curve of FE results for specimens compared with experimental results. In general, there was an acceptable convergence between FE and experimental curves. The load-deflection curves of (the FEA) analysis were stiffer than the experimental one in both the elastic and plastic zone. Generally, the FE mode of failure and actual failure mechanisms were in good agreement. The failure modes of FE analysis for the simulation specimen and in Plates (11-20).

Figure 15. Load mid-span deflection for beam B1-1

Table 5. The finite element analysis results

Specimens	Experimental results		Finite Element results		Δ P	ΔD
	Ultimate load (kN)	Max. mid-span deflection (mm)	Ultimate load (kN)	Max. mid-span deflection (mm)		
B1-1	205	32.91	211.6	32.77	3.2	0.43
B'1-1	210	27.54	221.2	27.49	5.3	0.18
B1-2	270	21.1	272.1	18.51	0.78	12.3
B1.5-0	170	33.78	178.85	34.4	5.2	1.8
B1.5-1	265	34.97	283.54	34.89	7	0.23
B '1.5-1	270	29.21	280.47	28.84	3.9	1.3
B1.5-2	340	36.74	361.43	36.76	6.4	0.05
B2-0	190	20.52	206.4	20.7	8.6	0.88
B2-1	290	35.42	310	36.45	6.9	2.9
B2-2	380	42.1	390	41.77	2.6	0.78
Average percentage difference					5 %	2.1 %

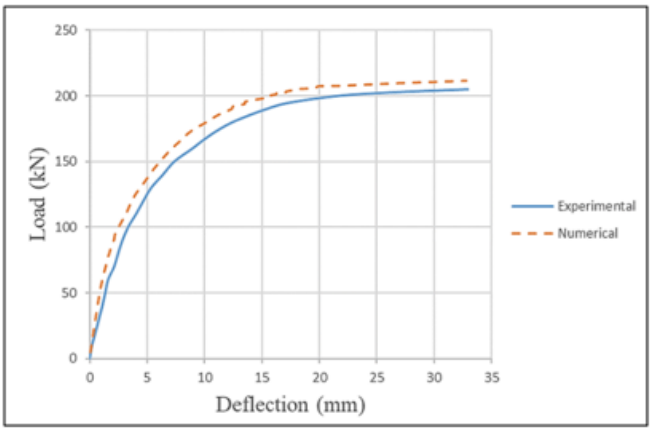

Figure 15. Load mid-span deflection for beam B1-1

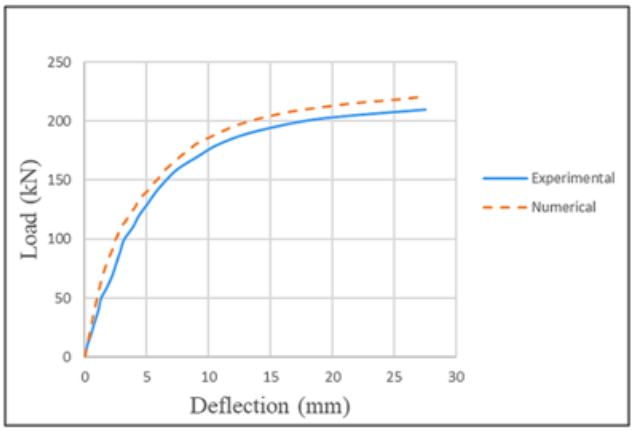

Figure 16. Load mid-span deflection for beam B'1-1

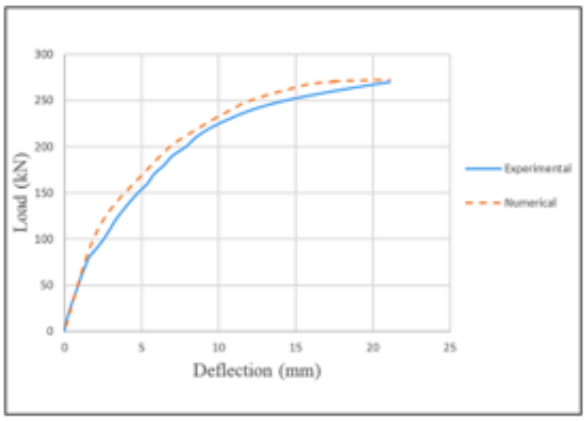

Figure 17. Load mid-span deflection for beam B1-2

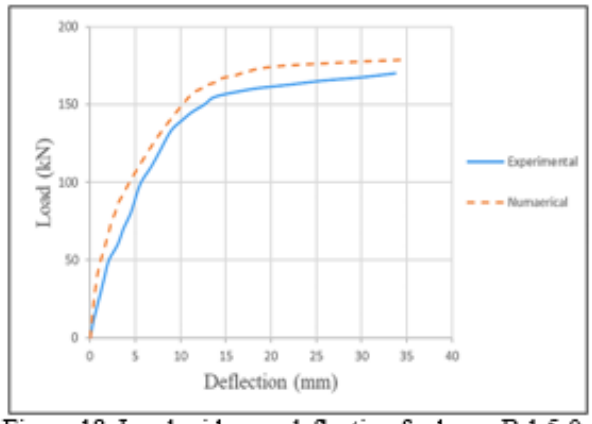

Figure 18. Load mid-span deflection for beam B 1.5-0

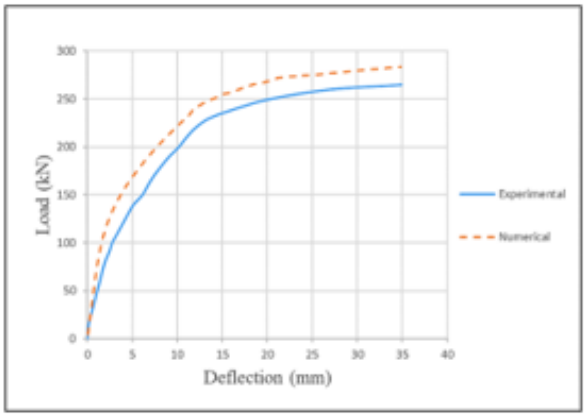

Figure 19. Load mid-span deflection for beam B 1.5-1

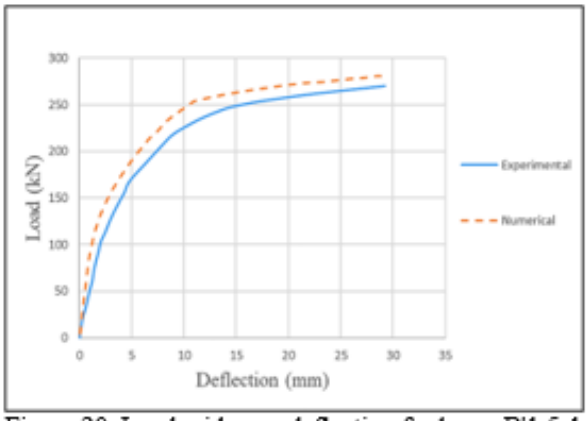

Figure 20. Load mid-span deflection for beam B'1.5-1

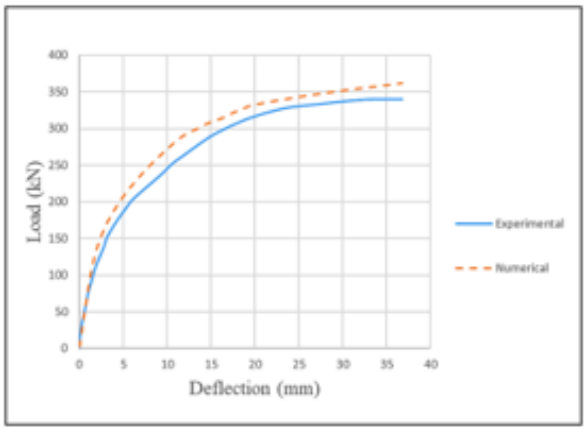

Figure 21. Load mid-span deflection for beam B1.5-2

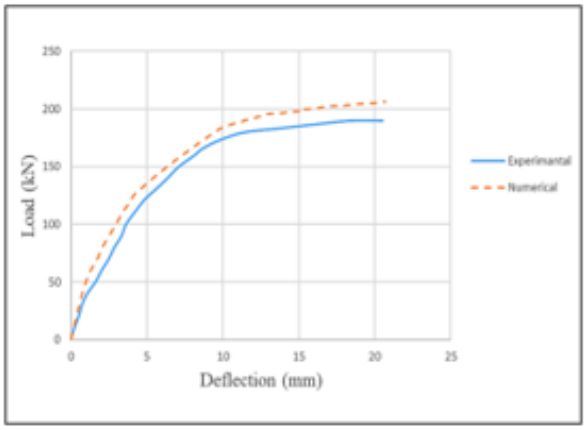

Figure 22. Load mid-span deflection for beam B2-0

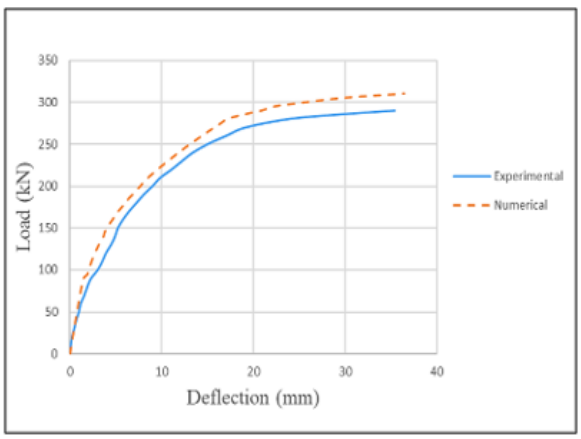

Figure 23. Load mid-span deflection for beam B2-1

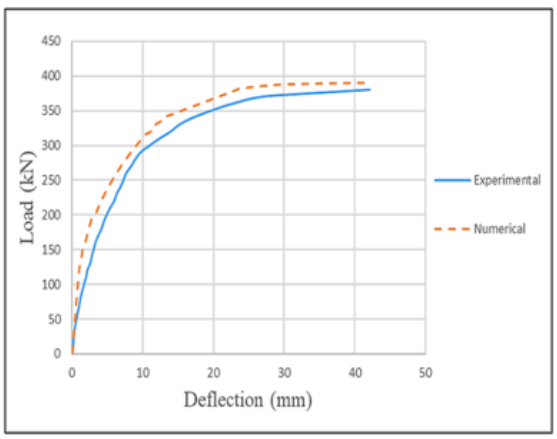

Figure 24. Load mid-span deflection for beam B2-2

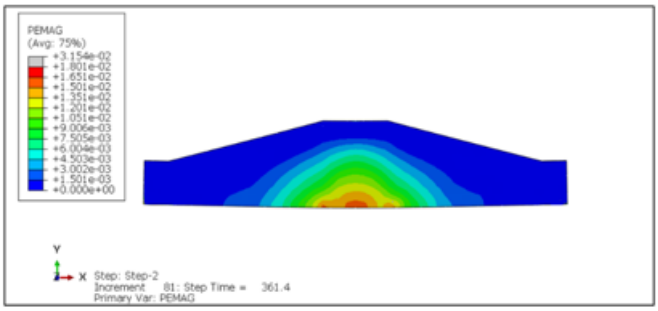

Plate 11. Mode of failure of the beam (B1-1)

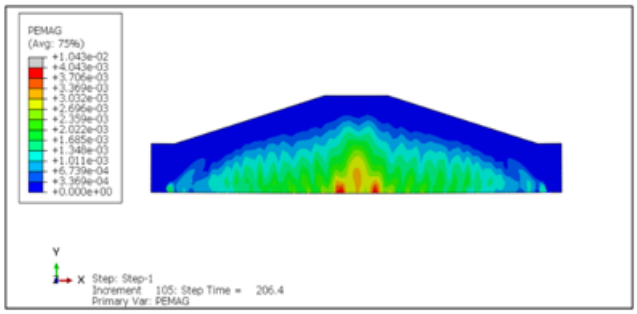

Plate 12. Mode of failure of the beam (B'1-1)

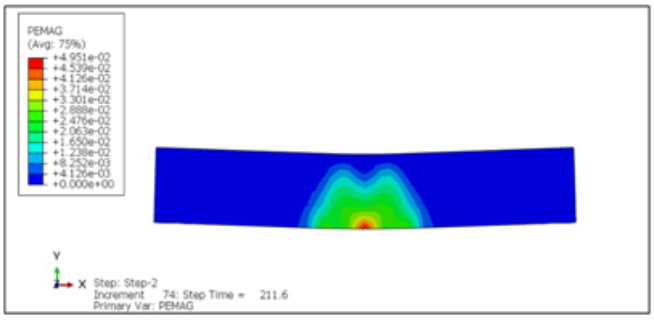

Plate 13. Mode of failure of the beam (B1-2)

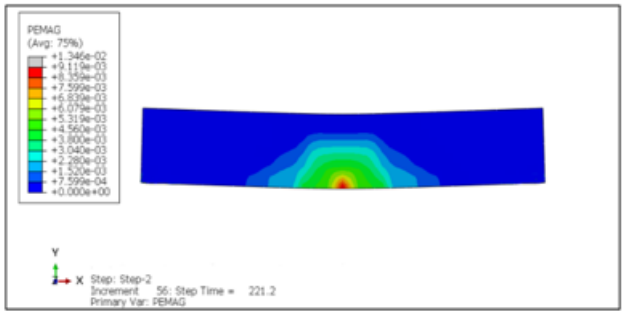

Plate 14. Mode of failure of the beam (B1.5-0)

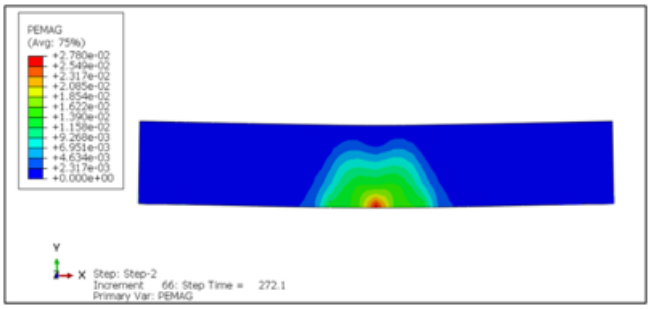

Plate 15. Mode of failure of the beam (B1.5-1)

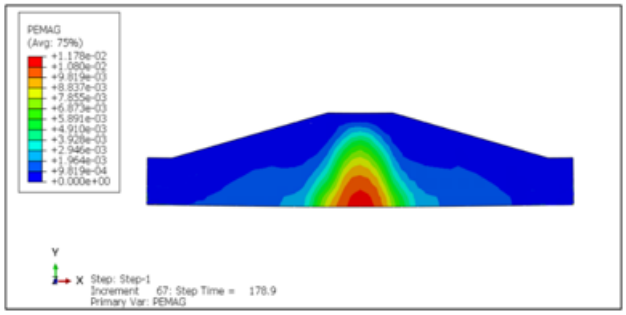

Plate 16. Mode of failure of the beam (B'1.5-1)

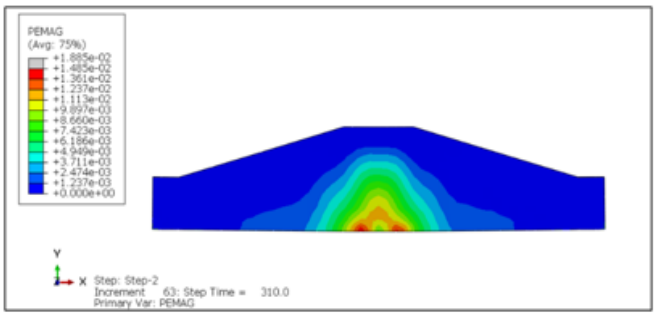

Plate 17. Mode of failure of the beam (B1.5-2)

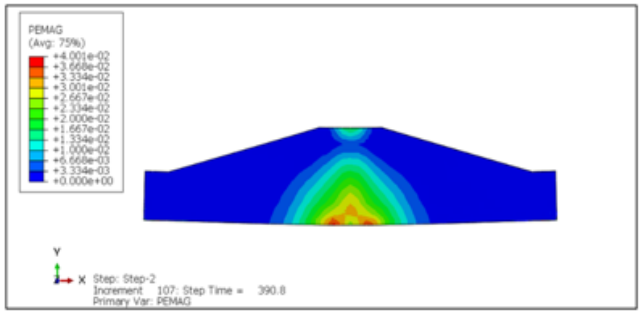

Plate 18. Mode of failure of the beam (B2-0)

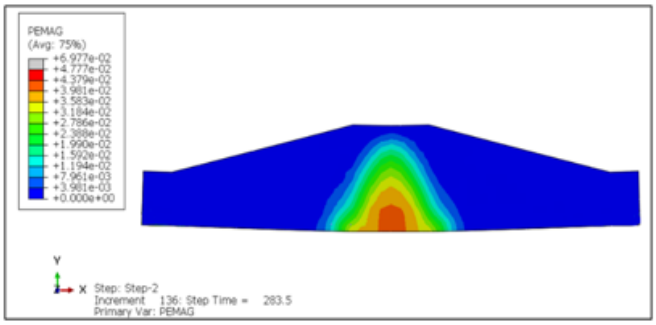

Plate 19. Mode of failure of the beam (B2-1)

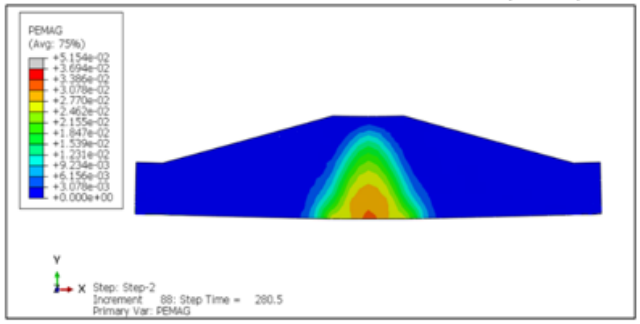

Plate 20. Mode of failure of the beam (B2-2)

4. Conclusions

The following are the main points that will serve as the present study conclusions: -

- Experimentally, it was found that changing the compressive strength from (40 MPa) to (55 MPa) will increase the cracking and ultimate load by (20% and 2.4%) for prismatic and by (12.5% and 1.9%) for non-prismatic beams, respectively.
- Adding a prestress reinforcement will impact the direction of the increase in the ultimate load between (52.63 to 55.88%) when putting one strand while putting two strands will raise the ultimate load by (100%) for both tapered beams.
- The results demonstrated that the increase in the tapering ratio would increase the ultimate load by no more than (29.27% and 41.46%) at beams with a tapering ratio of (1.5 and 2).
- According to the experimental study, the deflection is affected differently by the adopted parameters. The increase in the compressive strength from (40MPa) to (55MPa) has a significant effect on decreasing the ultimate deflection by (16.29% and 16.33%) for prismatic and non-prismatic beams, respectively. For the prismatic beam putting (two strands instead one) will decrease the ultimate moment by (35.87%). Additionally, in non-prismatic beams, when a tapering ratio is (1.5), putting (one and two) strands will increase the ultimate deflection by (3.25% and 8.58%), in order, while for the same approach but at a tapering ratio is (2), an increase in ultimate deflection can be observed by (34.5% and 105.2%). For beams that have (one strand), the increase in tapering ratio (to 1.5 and 2) will increase the ultimate deflection by (40.74% and 7.6%) for beams with a tapering ratio (1.5 and 2), respectively. Correspondingly, for beams having (two strands), the ultimate deflection will increase by (73.93% and 99.53%) when a tapering ratio is raised from (1 to 1.5 and 2), in that order.
- The results demonstrated a slight effect for increasing the concrete compressive strength in the direction of lowering the service deflection for both prismatic and non-prismatic (tapered) beams. In general, when it comes to tapered beams, the rise of prestressing reinforcement and tapering ratios impacts the service deflection in the direction of decline.
- The finite element modeling overvalues the ultimate load and deflection slightly in general compared with the experimental results. The numerical results showed a good correlation with the experimental data, which did not exceed (8.6% and 12.3%) for maximum load and deflection in order.

Declaration of competing interest

The authors declare that they have no recognized non-financial or financial competing interests in any materials conversed in the current work.

Funding

No funding was gained from any financial organization for conducting the current work.

References

[1] A. Jolly and V. Vijayan, "Structural behaviour of reinforced concrete haunched beam: A study on ANSYS and ETABS," *Int. J. Innovative Sci. Eng. Technol*, vol. 3, pp. 495-500, 2016.

[2] A. Tena-Colunga, "Concerns regarding the seismic design of reinforced concrete haunched beams," *Structural Journal*, vol. 91, pp. 287-293, 1994.

[3] A. Tena-Colunga, H. I. Archundia-Aranda, and Ó. M. González-Cuevas, "Behavior of reinforced concrete haunched beams subjected to static shear loading," *Engineering Structures*, vol. 30, pp. 478-492, 2008.

[4] A. Taoum, "Application of local post-tensioning to new and existing structures," University of Tasmania, 2016.

[5] E. Cross, "Post-tensioning in building structures," *Concrete in Australia*, vol. 33, pp. 48-54, 2007.

[6] H. I. Archundia-Aranda, A. Tena-Colunga, and A. Grande-Vega, "Behavior of reinforced concrete haunched beams subjected to cyclic shear loading," *Engineering Structures*, vol. 49, pp. 27-42, 2013.

[7] E. A. Godínez-Domínguez, A. Tena-Colunga, and G. Juárez-Luna, "Nonlinear finite element modeling of reinforced concrete haunched beams designed to develop a shear failure," *Engineering Structures*, vol. 105, pp. 99-122, 2015.
[8] T. Shuo, K. Okubo, and J. Niwa, "The shear behavior of RC tapered short beams with stirrups," *Journal of Advanced Concrete Technology*, vol. 17, pp. 506-517, 2019.
[9] H. Park, S. Jeong, S.-C. Lee, and J.-Y. Cho, "Flexural behavior of post-tensioned prestressed concrete girders with high-strength strands," *Engineering Structures*, vol. 112, pp. 90-99, 2016.
[10] C. HOU, T. NAKAMURA, T. IWANAGA, and J. NIWA, "Shear behavior of reinforced concrete and prestressed concrete tapered beams without stirrups," *Journal of JSCE*, vol. 5, pp. 170-189, 2017.
[11] D.-X. Xiong and X.-X. Zha, "A numerical investigation on the behaviour of concrete-filled steel tubular columns under initial stresses," *Journal of Constructional Steel Research*, vol. 63, pp. 599-611, 2007.
[12] R. Butola, Q. Murtaza, and R. M. Singari, "An experimental and simulation validation of residual stress measurement for manufacturing of friction stir processing tool," *Indian Journal of Engineering and Materials Sciences (IJEMS)*, vol. 27, pp. 826-836, 2021.
[13] T. D. Pham and W.-K. Hong, "Investigation of Strain Evolutions in Prestressed Reinforced Concrete Beams Based on Nonlinear Finite Element Analyses Considering Concrete Plasticity and Concrete Damaged Plasticity," *Journal of Asian Architecture and Building Engineering*, vol. 21, pp. 448-468, 2022.